Pergamon

Tetrahedron Vol. 51, No. 43, pp. 11775-11792, 1995

0040-4020/95 $9.50+0.00

0040-4020(95)00714-8

The Interaction of the 2'-OH Group with the Vicinal Phosphate in Ribonucleoside 3'-ethylphosphate Drives the Sugar-Phosphate Backbone into Unique (S,ε⁻) Conformational State

J. Plavec, C. Thibaudeau, G. Viswanadham, C. Sund, A. Sandström & J. Chattopadhyaya*

Department of Bioorganic Chemistry, Box 581, Biomedical Centre,
Uppsala University, S-751 23 Uppsala, Sweden

Dedicated to Professor Ivar Ugi on his 65th Birthday.

Abstract: *The analysis of temperature-dependent vicinal proton-proton coupling constants has shown that the North (N) ⇄ South (S) pseudorotational equilibria of ribonucleoside 3'-ethylphosphates [ApEt (**21**), GpEt (**22**), CpEt (**23**), rTpEt (**24**) and UpEt (**25**)], modelling simple diribonucleoside(3'→5')monophosphate without any intramolecular base-base stacking, are driven more towards the South-type sugar (S) by $\Delta\Delta H^\circ \approx$ -2.5 kJ mol^{-1} in the case of purine and by ≈ -3.8 kJ mol^{-1} in the case of pyrimidine nucleotides compared to the corresponding parent ribonucleosides **1** - **5**. In contrast, the S-type sugar conformation in 2'-deoxyribonucleoside 3'-ethylphosphates (ref. 3d) is stabilized by $\Delta\Delta H^\circ \approx$ -1.9 kJ mol^{-1} in both purine and pyrimidine nucleotides compared to the parent 2'-deoxyribonucleosides. The total energetic effect of 2'-OH group due to its interaction with the vicinal phosphate in ribonucleotides in contrast with the corresponding 2'-deoxynucleotide counterparts can be assessed by subtracting the free-energies of N ⇄ S pseudorotational equilibria in the ribonucleotide analogs **21** - **25** from the corresponding 2'-deoxynucleotide counterparts **16** - **20** : $\Delta\Delta G^{298} \approx$ +0.3 kJ mol^{-1} in ApEt (**21**), +0.6 kJ mol^{-1} in GpEt (**22**), +2.1 kJ mol^{-1} CpEt (**23**), +1.1 kJ mol^{-1} in rTpEt (**24**) and +1.3 kJ mol^{-1} in UpEt (**25**). The additional stabilization of the S-type pseudorotamers in ribonucleoside 3'-ethylphosphates **21** - **25** compared to ribonucleoside 3'-monophosphates **11** - **15** by $\Delta\Delta H^\circ \approx$ -2.0 kJ mol^{-1} is attributed to the influence of the 2'-OH group in the former. The population of ε' rotamers increases by 7-13% from 278 to 358K, which corresponds also with an equal increase of the population of N-type pseudorotamers, suggesting a unique cooperativity in the two-state (N,ε') ⇄ (S,ε⁻) conformational equilibria in **21** - **25**. These cooperative conformational transitions of (N,ε') ⇄ (S,ε⁻) equilibrium in **21** - **25** have been found to be orchestrated by the interaction of 2'-hydroxyl group with the vicinal phosphate as evident by the non-equivalent methylene protons of the 3'-ethylester function upto 348K in **21** - **25** compared to the 2'-deoxynucleotide counterparts **16** - **20** (ref. 3d). The intramolecular interaction of the 2'-OH function with the vicinal phosphodiester stabilizes the S and ε⁻ conformers ("On" switch), whereas 2'-OH in a non-interacting state stabilizes the N and ε' conformers ("Off" switch) in **21** - **25**. The strengths of this "On-Off" molecular switch for the preference of (S,ε⁻) conformational state over (N,ε') state in **21** - **25** are as follows: $\Delta G^{298} \approx$ -2.8 kJ mol^{-1} for adenosine 3'-ethylphosphate (**21**), -2.1 kJ mol^{-1} for guanosine 3'-ethylphosphate (**22**), ≈ 0.1 kJ mol^{-1} for cytidine 3'-ethylphosphate (**23**), -0.9 kJ mol^{-1} for ribothymidine 3'-ethylphosphate (**24**) and -0.7 kJ mol^{-1} for uridine 3'-ethylphosphate (**25**).*

The pentofuranose, the heterocycle and the phosphodiester are the essential three components that contribute to the dynamic and flexible architecture of nucleic acids. The pentofuranose moiety reduces its energy by becoming puckered (Scheme 1).[1,2] We have earlier shown that in solution various steric and stereoelectronic gauche and anomeric effects energetically drive the North (N) ⇄ South (S) sugar pseudorotational equilibrium.[3] In order to further understand the forces that govern the stabilization of the secondary structure of oligo- and polynucleotides we have designed and synthesised nucleoside 3'-ethylphosphates, which serve as simple model systems mimicking dinucleoside(3'→5')monophosphate. The essence of the conformational study with such simple model systems is that the effect of internucleotidyl base-

base stacking on the drive of the sugar-phosphate backbone is completely eliminated, thereby examining and dissecting the nature of fundamental intranucleotidyl interactions that contribute to the drive of the sugar-phosphate backbone in RNA. These simple model systems have allowed us for the first time to examine how the ribosugar conformation and the orientation of the constituent 2'-OH group influence the conformational preference of phosphate backbone torsions and *vice versa*.

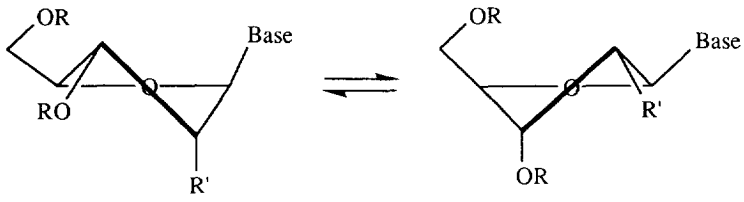

North sugar ($C_{3'}$-*endo*-$C_{2'}$-*exo*)
Phase angle (P) : $0° \leq P \leq 36°$;
Puckering amplitude (Ψ_m) : $30° \leq \Psi_m \leq 46°$

South sugar ($C_{2'}$-*endo*-$C_{3'}$-*exo*)
Phase angle (P) : $144° \leq P \leq 190°$;
Puckering amplitude (Ψ_m) : $30° \leq \Psi_m \leq 46°$

Base = adenine-9-yl (A), guanine-9-yl (G), cytosine-1-yl (C), thymine-1-yl (T) or uracil-1-yl (U)
R = H or phosphodiester moiety
R' = H or OH

Scheme 1: The dynamic two-state pseudorotational equilibrium of the β-D-pentofuranose moiety is determined by the nature and relative orientations of substituents. The involvement of 2'-OH in the gauche effects with O4', O3' and anomeric N atom as well as other intramolecular interactions are responsible for the conformational differences between DNA and RNA (see ref. 3).

Our recent work on a comparative conformational study on 3'-monophosphates **6** - **10** and 3'-ethylphosphates **16** - **20** of 2'-deoxynucleosides with the respective parent nucleosides has already shown[3d] that the gauche effects of 3'-monophosphate and 3'-ethylphosphate in 2'-deoxynucleotides drive the N ⇄ S equilibrium in an energetically very similar manner, and they both stabilize the S-type pseudorotamer by $\Delta H° \approx 1.7$ kJ mol^{-1} in comparison with 3'-OH group in the parent 2'-deoxynucleoside.[3d] In that study we did not observe any change in the population of ε and β rotamers of the phosphodiester moiety as a response to the shift of N ⇄ S dynamic equilibrium (4 - 9%) of the pentofuranose moiety as a function of temperature change from 278K to 358K. This led us to the conclusion that the processes of the conformational changes of the pentofuranose and the phosphodiester moieties in DNA are independent in the absence of base-base stacking.[3d]

We here report on the conformational study on ribonucleoside 3'-ethylphosphates **21** - **25** by the analysis of their temperature-dependent homo- and heteronuclear coupling constants and compare them with those of ribonucleosides **1** - **5** and their corresponding 3'-monophosphates **11** - **15**. This study has shed new light on the forces and their energetics which make the chemical reactivities and consequently the functional behavior of RNA so different from DNA. Data presented here show for the first time that the presence of 2'-OH has significant influence[4] on the thermodynamic stability of the preferred conformer of the pentofuranose and the phosphodiester moieties. Such 2'-OH promoted energetic preferences act as a molecular switch that cooperatively drives the puckering of the ribofuranose moiety along with the preferential rotamer distribution of the phosphate backbone torsions. This work is fully consistent with our earlier report[3g] where we unambiguously showed how the 2'-OH group in a ribonucleoside acts as a molecular switching device which can be turned on and off to drive N ⇄ S pseudorotational equilibria in a certain specific manner: In comparison with the 2'-deoxy counterparts, the strength of the gauche effect of the [O4'-C4'-C3'-3'OH] and [O4'-C4'-C3'-

3'OPO_3H^-] fragments stabilizing the N⇄ S equilibrium towards S is reduced by 2.2 kJ mol^{-1} in adenosine and by 3.1 kJ mol^{-1} in 3'-AMP, respectively, owing to a specific intramolecular 3'-OH····O2' hydrogen-bonding in the former[3g], and a more free 2'-OH in the latter.[3g]

Result and Discussion

Vicinal proton-proton ($^3J_{HH}$), proton-phosphorous ($^3J_{HP}$) and carbon-phosphorous ($^3J_{CP}$) coupling constants of β-D-ribopentofuranose moieties in **1** - **5** , **11** - **15** and **21** - **25** were measured in the range 278 K to 358 K in 10 K steps in D_2O (see Table 1 and experimental section). They were subsequently used to understand the interdependency of the conformational preferences of the pseudorotational equilibrium with those of the ε and β torsions of the constituent 3'-ethylphosphate moiety.

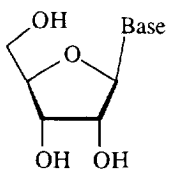

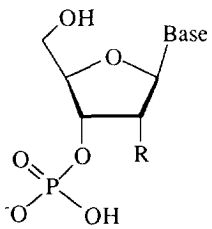

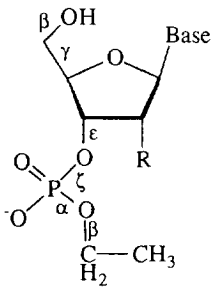

1: A	**6**: dAMP (R=H)	**11**: AMP (R=OH)	**16**: dApEt (R=H)	**21**: ApEt (R=OH)
2: G	**7**: dGMP (R=H)	**12**: GMP (R=OH)	**17**: dGpEt (R=H)	**22**: GpEt (R=OH)
3: C	**8**: dCMP (R=H)	**13**: CMP (R=OH)	**18**: dCpEt (R=H)	**23**: CpEt (R=OH)
4: rT	**9**: TMP (R=H)	**14**: rTMP (R=OH)	**19**: TpEt (R=H)	**24**: rTpEt (R=OH)
5: U	**10**: dUMP (R=H)	**15**: UMP (R=OH)	**20**: dUpEt (R=H)	**25**: UpEt (R=OH)

Base = adenine-9-yl (A), guanine-9-yl (G), cytosine-1-yl (C), thymine-1-yl (T), uracil-1-yl (U)

Scheme 2

(A) Estimation of temperature-dependent N ⇄ S pseudorotational equilibria. The experimental $^3J_{HH}$ were interpreted in terms of the two-state N ⇄ S conformational equilibrium[1-3] with the use of computer program PSEUROT (ver. 5.4).[5,6] Van't Hoff type analysis[3,6] of the temperature-dependent two-state N ⇄ S pseudotorational equilibrium[3] gave the enthalpy (ΔH°) and the entropy (ΔS°) values of the conformational equilibria in **1** - **5** , **11** - **15** and **21** - **25** (Fig. 1 and Table 2). Data in Table 2 show that at 298K the enthalpy contribution to the free-energy of the conformational equilibrium is stronger than entropy contribution in all compounds, but they are of equal strength in rT (**4**) and CpEt (**23**).

The pairwise subtraction of ΔH° values in ribonucleosides **1** - **5** from their corresponding 3'-monophosphates **11** - **15**, respectively [ΔΔH° values are: -0.3 kJ mol^{-1} for AMP (**11**), -1.3 kJ mol^{-1} for GMP (**12**), -1.7 kJ mol^{-1} for CMP (**13**), -2.2 kJ mol^{-1} for rTMP (**14**) and -0.9 kJ mol^{-1} for UMP (**15**)] shows that the S-type pseudorotamers are uniformly stabilized in the latter due to the stronger gauche effect of 3'-monophosphate compared to that of the 3'-OH (Table 2). Note, that this greater preference for the S-type

Table 1. Temperature variation of some $^3J_{HH}$, J_{HP} and $^3J_{CP}$ (in Hz)[a] coupling constants in **21** - **25**

Compound	Coupling constant	278K	288K	298K	308K	318K	328K	338K	348K	358K
ApEt (**21**)	$^3J_{H1'H2'}$	7.0	6.9	6.8	6.7	6.6	6.5	6.4	6.3	6.2
	$^3J_{H2'H3'}$	5.2	5.2	5.2	5.2	5.2	5.3	5,3	5.3	5.4
	$^3J_{H3'H4'}$	2.3	2.5	2.6	2.8	2.9	3.0	3.1	3.3	3.4
	$^3J_{C4'P}$	2.2	2.7	3.0	3.1	3.3	3.4	3.5	3.7	3.8
	$^3J_{C2'P}$	5.5	5.4	5.3	5.3	5.2	5.0	5.0	4.9	4.8
	$^3J_{H3'P}$	7.8	7.8	b	7.8	7.8	7.8	7.8	7.7	7.7
	$^3J_{CH_3P}$	7.1	7.1	7.0	6.9	6.7	6.7	6.7	6.6	6.7
	$^3J_{CH_2P}$	7.2	7.3	7.3	7.4	7.4	7.5	7.6	7.8	7.8
	$^3J_{CH_2P}$	7.0	7.0	7.1	7.2	7.3	7.4	7.4	7.2	7.1
	$^4J_{H2'P}$	1.5	1.5	1.5	1.4	1.4	1.3	1.2	1.1	1.0
GpEt (**22**)	$^3J_{H1'H2'}$	6.6	6.5	6.4	6.3	6.2	6.1	6.0	5.9	5.8
	$^3J_{H2'H3'}$	5.2	5.3	5.3	5.3	5.4	5.4	5.4	5.4	5.5
	$^3J_{H3'H4'}$	2.8	3.0	3.1	3.2	3.3	3.4	3.6	3.6	3.7
	$^3J_{C4'P}$	2.8	3.0	3.2	3.3	3.6	3.8	3.8	3.8	4.0
	$^3J_{C2'P}$	5.5	5.2	5.2	5.1	5.0	5.0	5.0	4.8	4.6
	$^3J_{H3'P}$	8.1	8.0	b	8.0	7.8	7.8	7.8	7.9	7.8
	$^3J_{CH_3P}$	7.0	7.0	6.9	6.7	6.7	6.8	6.8	6.7	6.5
	$^3J_{CH_2P}$	7.2	7.3	7.3	7.4	7.4	7.4	7.5	7.7	7.9
	$^3J_{CH_2P}$	6.8	7.1	7.1	7.1	7.3	7.4	7.4	7.3	7.3
	$^4J_{H2'P}$	1.2	1.2	1.3	1.2	1.1	1.2	1.2	1.2	1.1
CpEt (**23**)	$^3J_{H1'H2'}$	4.8	4.8	4.8	4.8	4.7	4.7	4.7	4.7	4.6
	$^3J_{H2'H3'}$	5.3	5.3	5.3	5.3	5.4	5.4	5.4	5.4	5.5
	$^3J_{H3'H4'}$	5.1	5.1	5.1	5.2	5.3	5.4	5.4	5.4	5.4
	$^3J_{C4'P}$	4.3	4.6	4.6	4.8	4.9	4.8	4.8	5.1	5.0
	$^3J_{C2'P}$	4.5	4.2	4.2	4.1	4.1	4.1	4.0	4.1	4.0
	$^3J_{H3'P}$	8.1	8.1	8.1	8.1	8.0	8.0	8.0	8.0	7.9
	$^3J_{CH_3P}$	7.3	7.0	6.7	6.8	6.9	6.7	6.8	6.7	6.8
	$^3J_{CH_2P}$	7.2	7.3	7.3	7.4	7.4	7.5	7.7	7.6	7.8
	$^3J_{CH_2P}$	6.9	7.1	7.1	7.2	7.4	7.4	6.7	7.0	7.0
rTpEt (**24**)	$^3J_{H1'H2'}$	5.6	5.6	5.6	5.5	5.5	5.5	5.4	5.4	5.3
	$^3J_{H2'H3'}$	5.5	5.5	5.5	5.5	5.5	5.5	5.5	5.5	5.6
	$^3J_{H3'H4'}$	4.2	4.3	4.3	4.5	4.6	4.6	4.7	4.7	4.8
	$^3J_{C4'P}$	3.8	4.1	4.3	4.3	4.3	4.4	4.5	4.6	4.8
	$^3J_{C2'P}$	4.6	4.8	4.6	4.6	4.6	4.5	4.3	4.2	4.3
	$^3J_{H3'P}$	8.2	8.1	8.1	8.0	8.0	8.0	7.9	8.0	7.8
	$^3J_{CH_3P}$	7.1	7.0	7.0	6.9	6.7	6.5	6.6	6.7	6.7
	$^3J_{CH_2P}$	7.2	7.2	7.3	7.4	7.4	7.5	7.5	7.6	7.7
	$^3J_{CH_2P}$	7.0	7.1	7.2	7.2	7.3	7.4	7.4	7.4	7.5
UpEt (**25**)	$^3J_{H1'H2'}$	5.4	5.4	5.3	5.3	5.3	5.3	5.2	5.2	5.1
	$^3J_{H2'H3'}$	5.4	5.4	5.5	5.5	5.5	5.6	5.5	5.6	5.6
	$^3J_{H3'H4'}$	4.5	4.6	4.6	4.6	4.7	4.8	4.8	4.8	4.8
	$^3J_{C4'P}$	4.0	4.2	4.2	4.4	4.4	4.6	4.6	4.7	4.7
	$^3J_{C2'P}$	4.7	4.8	4.7	4.6	4.6	4.5	4.5	4.4	4.4
	$^3J_{H3'P}$	8.1	8.1	8.0	8.0	8.0	7.9	7.9	7.9	7.8
	$^3J_{CH_3P}$	7.2	7.1	6.9	6.9	6.8	6.7	6.8	6.7	6.7
	$^3J_{CH_2P}$	7.2	7.3	7.3	7.4	7.4	7.5	7.5	7.6	7.7
	$^3J_{CH_2P}$	7.0	7.1	7.2	7.2	7.3	7.4	7.4	7.5	7.5
	$^4J_{H2'P}$	0.7	0.8	0.7	0.7	0.7	0.6	0.5	0.5	0.5

[a] See experimental section for the acuarcy of the measurements. [b] Intractable because of overlap with HOD signal

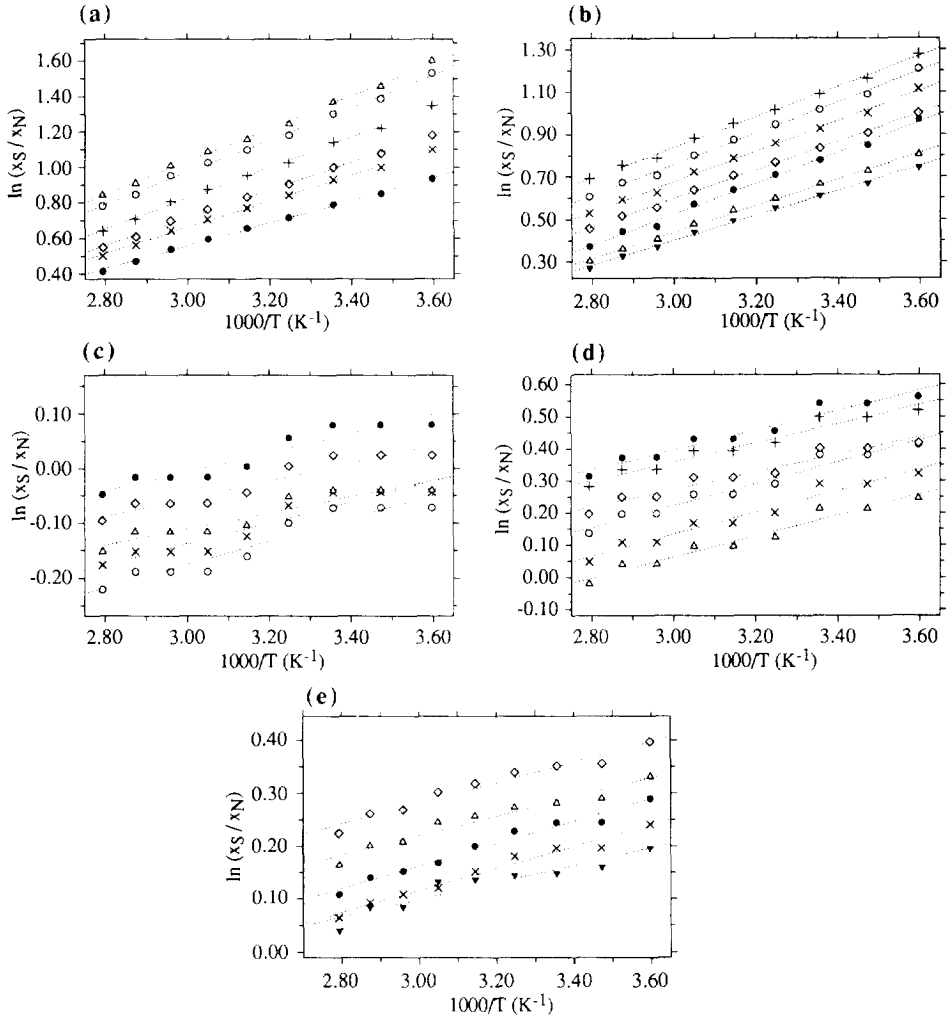

Figure 1. Van't Hoff plots of $\ln(x_S/x_N)$ as a function of 1000/T for ApEt (**21**) [panel (a)], GpEt (**22**) [panel (b)], CpEt (**23**) [panel (c)], rTpEt (**24**) [panel (d)] and UpEt (**25**) [panel (e)]. The least square fitted straight lines are based on the mole fractions of N (x_N) and S (x_S) pseudorotamers from many PSEUROT analyses[5,6] (for clarity only representative plots are shown): for ApEt (**21**) [panel (a)] Ψ_m of both N and S conformers were constrained to 31° (o) and 38° (×) and also the minor N-type pseudorotamers were constrained to P_N = -36°, Ψ_N = 29° (●), P_N = -36°, Ψ_N = 40° (◊), P_N = -18°, Ψ_N = 40° (△) and P_N = 36°, Ψ_N = 29° (+); for GpEt (**22**) [panel (b)] Ψ_m of both N and S conformers were constrained to 30° (o), 31° (×), 33° (●), 35° (◊) and 39° (△) and also the minor N-type pseudorotamers were constrained to P_N = 18°, Ψ_N = 33° (+), P_N = -36°, Ψ_N = 33° (▼); for CpEt (**23**) [panel (c)] Ψ_m of both N and S conformers were constrained to 30° (o), 33° (×), 35° (●), 37° (◊) and 39° (△); for rTpEt (**24**) [panel (d)] Ψ_m of both N and S conformers were constrained to 30° (o), 31° (×), 33° (●), 37° (◊), 39° (△) and 40° (+); for UpEt (**25**) [panel (e)] Ψ_m of both N and S conformers were constrained to 30° (●) 31° (×), 34° (◊), 36° (△) and 40° (▼) (see ref. 6 for details). Individual enthalpy (ΔH°) and entropy (ΔS°) values were derived from the slopes and intercepts respectively of each van't Hoff plot according to the relation $\ln(x_S/x_N) = -(\Delta H°/R)(1000/T) + \Delta S°/R$ and were used subsequently to calculate average ΔH° and ΔS° contributions to the N ⇄ S pseudorotational equilibria of **21** - **25** (Table 2).

Table 2: Thermodynamic data of the N⇄ S pseudorotational equilibria in **1** - **5**, **11** - **15** and of the (N,ε^t) ⇄ (S,ε$^-$) conformational equilibria in **21** - **25**

Compound	Estimation of the drive of N ⇄ S pseudorotational equilibria derived from temperature-dependent $^3J_{HH}$						
	$\Delta H°$ [a]	$\Delta S°$ [a]	$-T\Delta S°$ [b]	ΔG^{298} [a]	$\%S^{278}$ [c]	$\%S^{358}$ [c]	$\Delta\%S$ [d]
A (**1**)	-4.6 (0.4)	-9.5 (0.6)	2.8	-1.8	70	60	-10
G (**2**)	-3.2 (0.2)	-5.5 (0.7)	1.6	-1.6	67	60	-7
C (**3**)	2.5 (0.2)	3.9 (0.9)	-1.2	1.3	35	41	+6
rT (**4**)	1.3 (0.1)	4.4 (0.7)	-1.3	0.0	49	52	+3
U (**5**)	2.1 (0.2)	6.2 (2.7)	-1.8	0.3	46	51	+5
AMP (**11**)[e]	-4.9 (0.4)	-9.1 (0.7)	2.7	-2.2	74	63	-11
GMP (**12**)	-4.5 (0.2)	-10.8 (1.6)	3.2	-1.3	66	55	-11
CMP (**13**)	0.8 (0.2)	-0.6 (1.8)	0.2	1.0	40	42	+2
rTMP (**14**)	-0.9 (0.2)	-1.6 (0.9)	0.5	-0.4	55	53	-2
UMP (**15**)	1.2 (0.2)	2.1 (1.2)	-0.6	0.6	43	46	+3
ApEt (**21**)	-6.9 (0.8)	-13.6 (1.1)	4.1	-2.8	79	66	-13
GpEt (**22**)	-5.8 (0.4)	-12.3 (1.1)	3.7	-2.1	74	62	-12
CpEt (**23**)	-1.5 (0.2)	-5.3 (1.0)	1.6	0.1	50	47	-3
rTpEt (**24**)	-2.5 (0.3)	-5.3 (1.2)	1.6	-0.9	61	55	-6
UpEt (**25**)	-1.6 (0.1)	-3.1 (0.6)	0.9	-0.7	58	54	-4
	Estimation of the drive of ε^t ⇄ ε$^-$ conformational equilibria derived from temperature-dependent $^3J_{HP}$ and $^3J_{CP}$						
	$\Delta H°_\varepsilon$ [a]	$\Delta S°_\varepsilon$ [a]	$-T\Delta S°$ [b]	ΔG^{298} [a]	$\%\varepsilon^{-278}$ [c]	$\%\varepsilon^{-358}$ [c]	$\Delta\%\varepsilon^-$ [f]
ApEt (**21**)	-6.6 (0.9)	-14 (3)	4.2	-2.4	76	63	-13
GpEt (**22**)	-5.8 (0.9)	-12 (3)	3.6	-2.2	74	62	-12
CpEt (**23**)	-2.8 (0.9)	-9 (4)	2.7	-0.1	53	46	-7
rTpEt (**24**)	-3.8 (0.8)	-8 (3)	2.4	-1.4	66	58	-8
UpEt (**25**)	-3.3 (0.7)	-7 (2)	2.1	-1.2	64	57	-7

[a] $\Delta H°$ (kJ mol^{-1}) and $\Delta S°$ (J mol^{-1} K^{-1}) are the average values (standard deviations are given in brackets) and were calculated from individual van't Hoff plots using populations of N and S pseudorotamers from several individual PSEUROT analyses. $\Delta H°_\varepsilon$ and $\Delta S°_\varepsilon$ were calculated from 15 van't Hoff plots using populations of ε^t and ε$^-$ rotamers. The signs of thermodynamic parameters are arbitrarily chosen in such a way that the positive values indicate the drive of N⇄ S and ε^t ⇄ ε$^-$ equilibria to N and ε^t, whereas the negative signs describe the drive to S and ε$^-$, respectively. ΔG^{298} are given at 298 K in units of kJ mol^{-1}. [b] $-T\Delta S°$ (kJ mol^{-1}) term is given at 298 K. [c] The population of the S and ε$^-$ conformers were calculated using the relation: %S (T) or %ε$^-$ (T) = 100 * [exp (- ΔG^T/ RT)] / [exp (- ΔG^T/ RT) +1]. [d] $\Delta\%S = \%S^{358} - \%S^{278}$. [e] $\Delta H°$ and $\Delta G°$ have been found to be pH invariant over the pH range from 6.5 to 8.4 (0.5 pH unit resolution). [f] $\Delta\%\varepsilon^- = \%\varepsilon^{-358} - \%\varepsilon^{-278}$.

pseudorotamers in **11**- **15** is dependent on the nature of the heterocyclic base: it is larger in the case of pyrimidine ($\Delta\Delta H°$ = -0.9 to -2.2 kJ mol^{-1}) than purine ($\Delta\Delta H°$ = -0.3 and -1.3 kJ mol^{-1}). In a similar manner, the subtraction of $\Delta H°$ for **1** - **5** from the 3'-ethylphosphate derivatives **21** - **25** (Table 2), respectively, gives the relative strength ($\Delta\Delta H°$) of gauche effect of O4'-C4'-C3'-3'OPO_3Et^- fragment in comparison to O4'-C4'-C3'-3'OH: -2.3 kJ mol^{-1} for ApEt (**21**), -2.6 kJ mol^{-1} for GpEt (**22**), -4.0 kJ mol^{-1} for CpEt (**23**), -3.8 kJ mol^{-1} for rTpEt (**24**) and -3.7 kJ mol^{-1} for UpEt (**25**). Therefore, the gauche effect of 3'-OPO_3Et^- moiety also drives the

sugar conformation towards S-type more effectively than 3'-OH group. Note, however, that the drive of N ⇄ S pseudorotational equilibria by 3'-monophosphate in **11** - **15** and 3'-OPO_3Et^- in **21** - **25** towards S in the ribonucleotides are not of comparable strengths in contrast to our earlier observation in 2'-deoxy counterparts (*vide infra*).[3d] The subtraction of ΔH° values in phosphomonoesters **11** - **15** from phosphodiesters **21** - **25**, respectively shows that 3'-OPO_3Et^- group additionally stabilizes the S-type pseudorotamers by: -2.0 kJ mol^{-1} for ApEt (**21**), -1.3 kJ mol^{-1} for GpEt (**22**), -2.3 kJ mol^{-1} for CpEt (**23**), -1.6 kJ mol^{-1} for rTpEt (**24**) and -2.8 kJ mol^{-1} for UpEt (**25**). It is noteworthy that the dissection of the energetics of interaction of 2'-hydroxyl group with the vicinal 3'-ethylphosphate from the other 2'-OH promoted gauche effects has also been independently possible from the two following comparisons[24] and led to the same conclusion : (i) comparison between the pairs of ribonucleoside-3'-ethylphosphates **21** - **25** and their 2'-deoxy counterparts **16** - **20**; and (ii) comparison between the pairs of ribonucleoside-3'-monophosphates **11** - **15** and their 2'-deoxy counterparts **6** - **10**.

Nucleoside 3'-monophosphates at neutral pH would be expected to have net charge of -1 ($pK_a \approx 1.5$ for the first dissociation of monophosphate) and -2 ($pK_a \approx 6.7$ for the second dissociation of monophosphate) in approximately 1 : 1 ratio, whereas the corresponding 3'-ethylphosphates are present with the net charge of -1 only. In our earlier study[3d] on 2'-deoxynucleoside-3'-monophoshates **6** - **10** and the corresponding 3'-ethylphosphates **16** - **20**, we have shown that the 3'-monophoshate and 3'-ethylphosphate at the neutral pH stabilize the S-type conformers with the quite comparable strengths [$\Delta\Delta H^\circ$ = (ΔH° of gauche effect of O4-C4'-C3'-monophosphate) – (ΔH° of gauche effect of O4-C4'-C3'-ethylphosphodiester) = 0.4 kJ mol^{-1}, $\sigma = 0.3$[3i]], which has been verified on five pairs of 2'-deoxy-3'-monophosphate and the corresponding 2'-deoxy-3'-ethylphosphate derivatives of A, G, C, T, U.[3] This comparative study[3d] clearly testifies one important point regarding the lack of influence of pH of the medium used for the NMR measurements for the determination of gauche effects: Although the gauche effect determined for 2'-deoxynucleoside-3'-monophosphates **6** - **10** at the neutral pH is the result of ~1:1 mixture of -1 and -2 charged phosphomonoester species, whereas the gauche effect in 2'-deoxy-3'-ethylphosphates **16** - **20** involve a monoanionic species under the condition of NMR measurement, yet the gauche effect of the 3'-ethylphosphodiester moiety in 2'-deoxy-3'-ethylphosphates is quite comparable to the gauche effect of the 3'-monophosphate moiety in 2'-deoxynucleoside-3'-monophosphates at the neutral pH. Furthermore, we have also performed the pH-dependent (pH 6.5 to 8.4, 0.5 pH unit resolution) $^3J_{HH}$ and $^3J_{HP}$ analysis on AMP **11**, as an example, at a wide temperature range in order to see if the change of net charge on nucleoside 3'-monophosphates in this pH range would have any effect on the strength of stabilization of any specific conformer. We find that $^3J_{HH}$ and $^3J_{HP}$ (from 278 - 358K) remain constant over the whole pH range from pH 6.5 to 8.4. Hence the ionization state of the 3'-monophosphate group does <u>not</u> affect the strength of the stabilization of S conformer by [O4'-C4'-C3'-phosphate] gauche effect. *This means that whatever additional stabilization of the S-type conformers in ribonucleoside 3'-ethylphosphates **21** - **25** compared to 3'-monophosphates **11** - **15** have been found[23] above should be attributed to the effect of vicinal 2'-hydroxyl function in ribonucleotides **21** - **25**.*

Independent of the above argument, the relative strengths of gauche effects of phosphates drawn on the basis of comparison of 3'-ethylphosphates **21** - **25** compared to 3'-monophosphates **11** - **15** have been furthermore corroborated by the comparative study[24] on the energetics for 3'-OPO_3Et^- derivatives of ribonucleosides **21** - **25** and 2'-deoxy counterparts **16** - **20**.

(B) Estimation of ε and β rotamer distribution of the 3'-ethylphosphate moiety. The experimental proton-phosphorous ($^3J_{HP}$) and carbon-phosphorous coupling constants ($^3J_{CP}$) in **21** - **25** were used for the

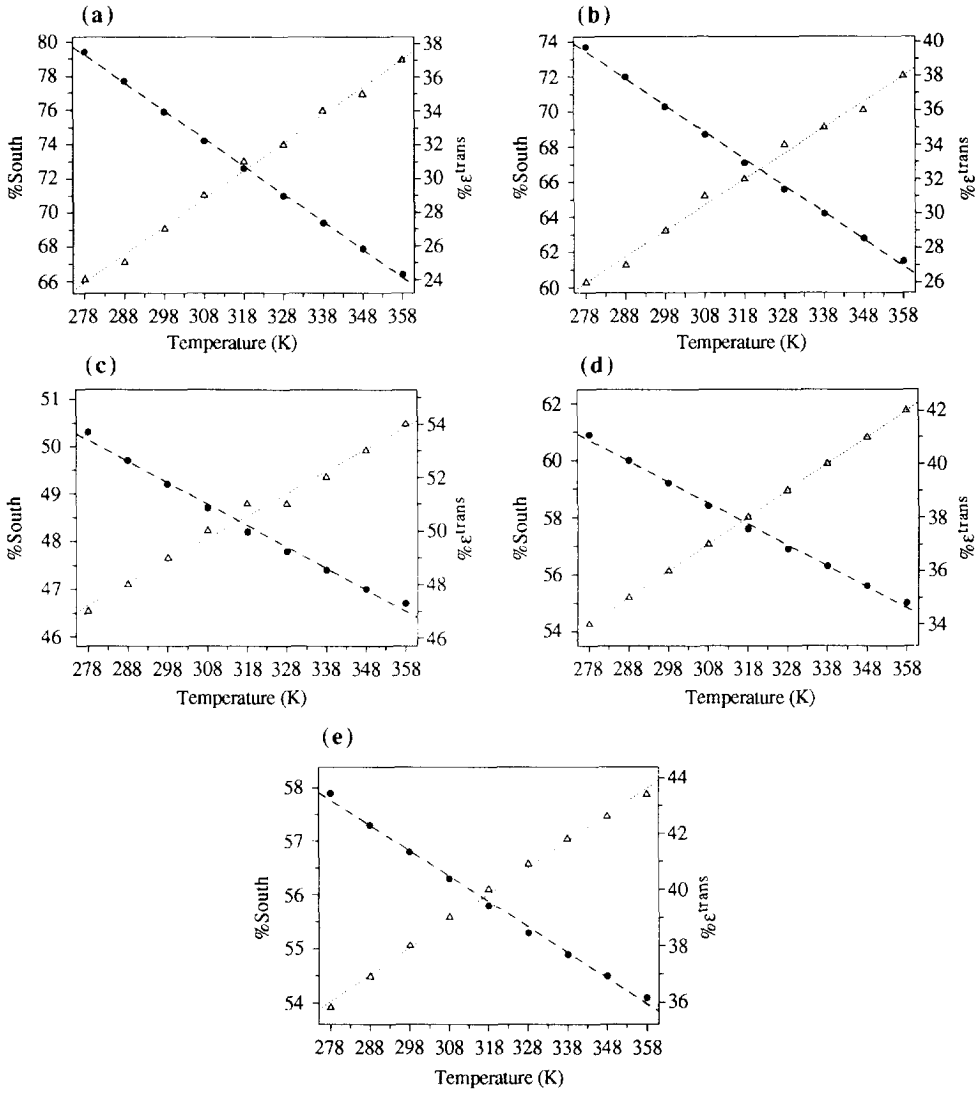

Figure 2. The population of the S-type pseudorotamers [dashed (---) line] and ε^t rotamers [dotted (····) line] as a function of temperature for ApEt (**21**) [panel (a)], GpEt (**22**) [panel (b)], CpEt (**23**) [panel (c)], rTpEt (**24**) [panel (d)] and UpEt (**25**) [panel (e)]. The %S at nine temperatures in the range 278 - 358 K were calculated from ΔH° and ΔS° values for N $\rightleftarrows$ S pseudorotational equilibria in **21** - **25** (Table 2) and are labeled with ● (points are connected with --- line). The $\%\varepsilon^t$ in the same temperature range were calculated from $\Delta H^\circ_\varepsilon$ and $\Delta S^\circ_\varepsilon$ values for $\varepsilon^t \rightleftarrows \varepsilon^-$ conformational equilibria in **21** - **25** (Table 2) and are labeled with △ (points are connected with ···· line). It is noteworthy that the decrease in %S population always promotes a corresponding increase in $\%\varepsilon^t$ population or likewise the increase of %N population promotes decrease in $\%\varepsilon^-$ population. Hence a two-state $(N,\varepsilon^t) \rightleftarrows (S,\varepsilon^-)$ conformational equilibrium in **21** - **25** is proposed.

determination of the torsion angle ε[C4'-C3'-O3'-P], which requires the knowledge of three coupling constants $^3J_{C4'P}$, $^3J_{C2'P}$ and $^3J_{H3'P}$ (Table 1).[7] Additionally, we have also used $^4J_{H2'P}$ to qualitatively assess[8] the population of ε⁻ rotamers.[9] The three-parameter Karplus equations[10,11] for $^3J_{CP} = 9.1 \cos^2\Phi - 1.9 \cos\Phi + 0.8$ and $^3J_{HP} = 15.3 \cos^2\Phi - 6.2 \cos\Phi + 1.5$ were used. Two-state $\varepsilon^t \rightleftarrows \varepsilon^-$ conformational equilibrium across C3'-O3' has been assumed in the present work in the interpretation of temperature-dependent $^3J_{C4'P}$, $^3J_{C2'P}$ and $^3J_{H3'P}$ coupling constants because of the following reasons: (i) X-ray studies have shown that in the solid state only trans (ε^t) and gauche⁻ rotamer (ε^-) occur, thereby indicating that ε^+ rotamer is "forbidden"[7a]; (ii) since the expected $^3J_{H3'P}$ for the ε^+ rotamer should be in the region of ≈23 Hz[7a,11] but the observed $^3J_{H3'P}$ is found to be 7-8 Hz, the high population of ε^+ is also unlikely in solution; (iii) a simple model building study along with classical potential function calculations[12] has shown that the phosphoryl-oxygen and O4' in ε^+ mode are in closer contact promoting a stronger steric and electrostatic repulsion than in ε^- or ε^t mode. The two-state $\varepsilon^t \rightleftarrows \varepsilon^-$ conformational equilibrium was assessed with our computer program EPSILON (see experimental section) which calculates the best fit of the experimental coupling constants with ε^t and ε^- torsion angles and their respective populations[13]. In this algorithm, the assumption has been made that with the change of temperature the $\varepsilon^t \rightleftarrows \varepsilon^-$ equilibrium is shifted, whereas the values of the ε torsion angles in both trans and gauche-minus ranges remain constant. The change in the population of ε^t rotamers in **21** - **25** as the function of temperature is presented in Fig. 2.

Fig. 2 shows that as the population of ε^t rotamers increases over ε^- rotamers, the population of S-type sugar conformers decreases with respect to N as the temperature increases from 278 K to 358 K. This showed that an increase of the population of ε^t rotamers corresponds to an identical increase in the population of N-type sugars at any temperature (Fig. 2). Similarly, it was also observed that when the increase of the population of ε^- rotamers takes place, it always corresponds with a comparable increase of S-type sugars (Fig. 2). This suggests that the sugar repuckering and the rotation around C3'-O3' in **21** - **25** are indeed mutually correlated and involved in the two-state $(N,\varepsilon^t) \rightleftarrows (S,\varepsilon^-)$ conformational equilibrium. The populations of the ε^t and ε^- rotamers at nine different temperatures were used to calculate the enthalpy ($\Delta H^\circ_\varepsilon$) and the entropy ($\Delta S^\circ_\varepsilon$) of the $\varepsilon^t \rightleftarrows \varepsilon^-$ conformational equilibrium in **21** - **25** through van't Hoff plots of [ln ($X\varepsilon^-$ / $X\varepsilon^t$)] vs. 1/T (Fig. 3 and Table 2).

Noteworthy are the ΔH° and ΔS° values for the N ⇄ S equilibrium, which were calculated from the temperature variation of sugar endocyclic $^3J_{HH}$ in **21** - **25** are quite similar to the $\Delta H^\circ_\varepsilon$ and $\Delta S^\circ_\varepsilon$ values for the $\varepsilon^t \rightleftarrows \varepsilon^-$ equilibrium calculated from the temperature variation of $^3J_{C4'P}$, $^3J_{C2'P}$ and $^3J_{H3'P}$ (Table 2). This means that the forces that govern the N⇄ S and the $\varepsilon^t \rightleftarrows \varepsilon^-$ equilibria in **21** - **25** are very similar. This is also consistent with our observation that the shift of N ⇄ S equilibrium (Δ%S) with the change in temperature from 278 K to 358 K is comparable to the shift of $\varepsilon^t \rightleftarrows \varepsilon^-$ equilibrium ($\Delta\%\varepsilon^-$) at identical temperature range. The very small discrepancies of only upto 4% units between the magnitudes of Δ%S and $\Delta\%\varepsilon^-$ shown in Table 2 are due to inaccuracies involved in the interpretation of coupling constants, especially when there is no bias to one type of conformers in the two-state equilibrium, and offer an additional proof of the cooperativity between sugar repuckering and rotation across C3'-O3' (ε torsion).

We have then explored how this cooperative conformational transition of $(N,\varepsilon^t) \rightleftarrows (S,\varepsilon^-)$ equilibrium is uniquely orchestrated by the intramolecular interaction involving the participation of 2'-OH group in **21** - **25** by molecular model building. It is clear that the different possibilities that one should consider for the involvement of 2'-hydroxyl group in the interaction either with O3' or one of the 3'-phosphate oxygens should not violate

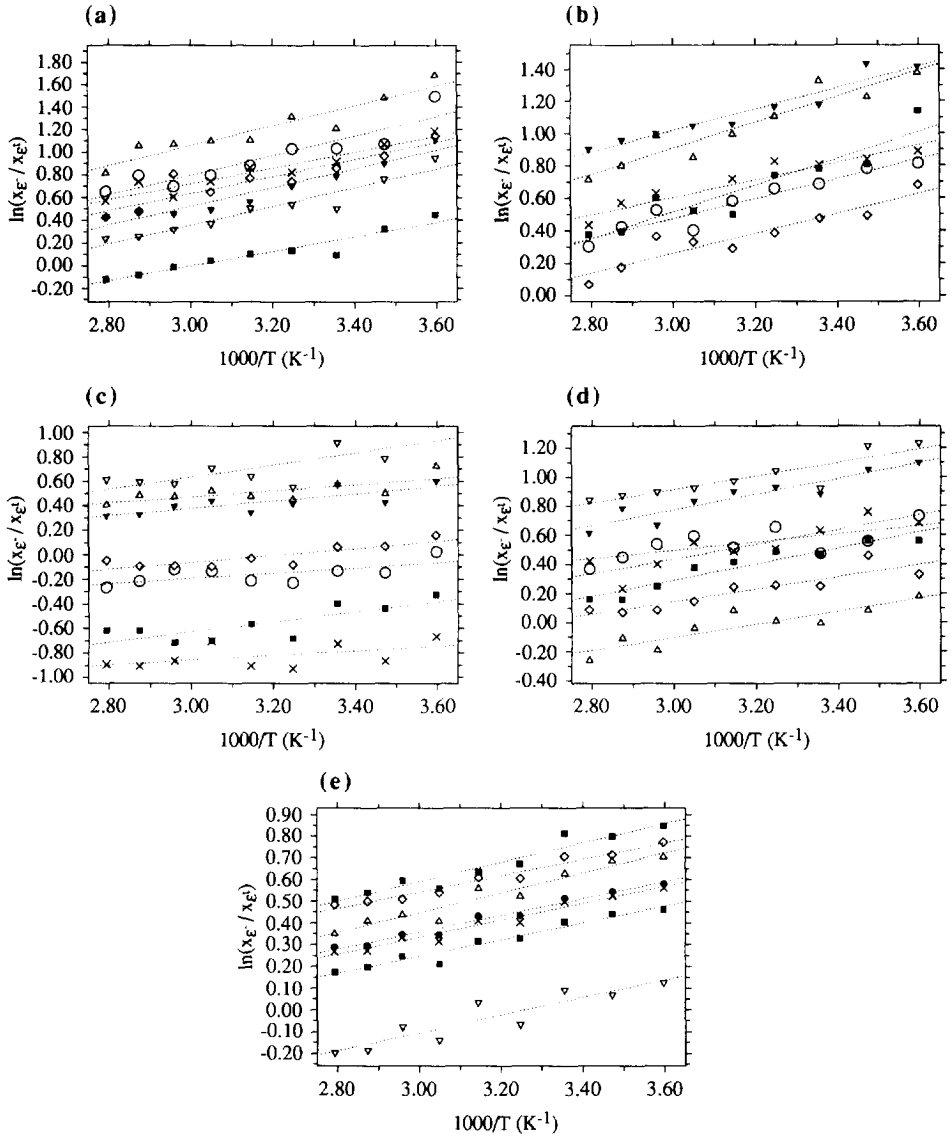

Figure 3. Van't Hoff plots of ln ($x_{\varepsilon^-}/x_{\varepsilon^1}$) (see text for the arguments favoring the two state $\varepsilon^1 \rightleftarrows \varepsilon^-$ equilibrium) as a function of 1000/T for ApEt (**21**) [panel (a)], GpEt (**22**) [panel (b)], CpEt (**23**) [panel (c)], rTpEt (**24**) [panel (d)] and UpEt (**25**) [panel (e)]. The least square fitted straight lines are based on the mole fractions of ε^- (x_{ε^-}) and ε^1 (x_{ε^1}) pseudorotamers from 15 calculations with our program EPSILON[13] (for clarity only representative plots are shown). Individual enthalpy ($\Delta H^\circ_\varepsilon$) and entropy ($\Delta S^\circ_\varepsilon$) values were derived from the slopes and intercepts respectively of each van't Hoff plot according to the relation ln ($x_{\varepsilon^-}/x_{\varepsilon^1}$) = - ($\Delta H^\circ_\varepsilon$ /R) (1000/T) + $\Delta S^\circ_\varepsilon$ /R and were subsequently used to calculate average $\Delta H^\circ_\varepsilon$ and $\Delta S^\circ_\varepsilon$ contributions to the $\varepsilon^1 \rightleftarrows \varepsilon^-$ conformational equilibria of **21** - **25** (Table 2).

the experimental observation of a specific ε⁻ orientation across C3'-O3' bond in preferred S-type puckering mode of the ribofuranose moiety.

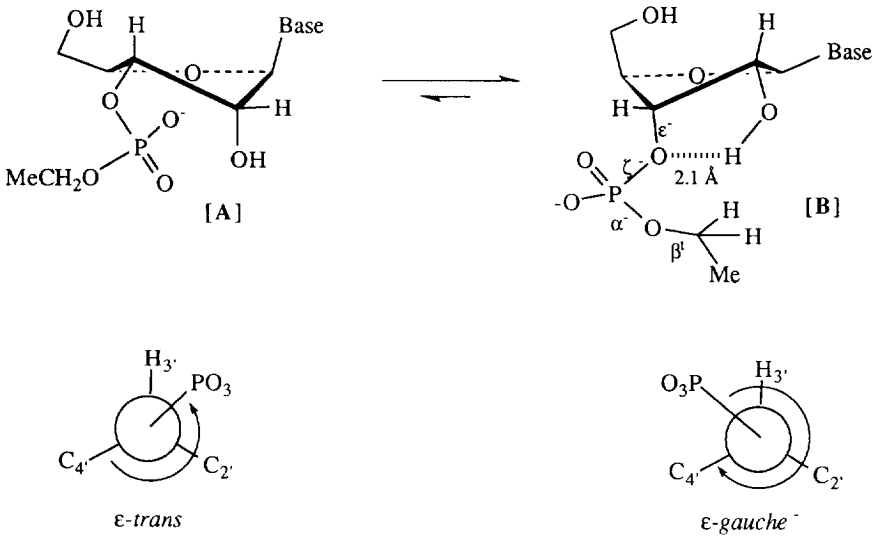

Scheme 3: Relative orientations of 3'-ethylphosphate and 2'-OH groups in (N,ε^t) [**A**]⇄ (S,ε$^-$) [**B**] conformational equilibrium in model compounds **21** - **25**.

We first considered if the 2'-OH could be H-bonded to the vicinal O3' (2'-OH····O3' distance is 2.1 Å) in S,ε$^-$ mode (Fig. B with ζ$^-$,α$^-$ and β^t state of the phosphate backbone in combination with (S,ε$^-$) state, on the basis of our molecular mechanics study,[21d] is shown in Scheme 3). Apparently, this is a long H-bonded bridge and the 2'-O-H···O3' H-bond angle would have to be considerably smaller than usual because of the fused nature of H-bonded ring with the furanose ring. In fact, intramolecular O-3'····O-2' H-bonds are not commonly found in nucleoside structures specially at the neutral state because the geometrical requirements are not fulfilled.[22a] There are however four possible reasons to consider the existence of a potential 2'-OH····O3' H-bonded bridge in **21** - **25**: First, there are a few examples of X-ray structures of nucleosides wherein the O-H····O distances have been found to vary between 1.74 and 2.20Å[1,22], for example, in inosine[22b] [d(2'-OH····O3')] = 2.1Å, O-H····O angle ≈ 147°; isodeazatubercidin[22c] [d(3'-OH····O2')] = 1.97Å, O-H····O angle = 131°; 6-amino-10-(β-D-ribofuranosylamino)pyrimido[5,4-*d*]pyrimidine[22d] [d(3'-OH····O2')] = 1.78Å, O-H····O angle = 154°. Second, the relatively high acidity of *cis*-2',3'-hydroxyls ($pK_a \approx 12.5$)[22e] in ribonucleosides has been ascribed to the ability of these hydroxyls to form intramolecular H-bond. It has been also shown that the substitution of 2'-OH by H as in 2'-deoxynucleosides causes a loss of acidity.[22e] Third, the effect of 2'-OH on the conformational preferences of phosphate torsions in **21** - **25** is also evident from the non-isochronous methylene protons of 3'-ethylphosphate groups compared to 2'-deoxynucleoside counterparts **16** - **20** (Fig. 4). It is noteworthy that as the temperature is increased to 358 K the methylene protons of ethyl ester group become near-isochronous because of the weakening of the interaction of 2'-OH with any of the vicinal heteroatom(s) (Fig. 4). In fact, the methylene protons of the ribonucleotide analogs at > 348 K become isochronous (see panels A3, B3, C3, D3 & E3 of Fig. 4 for spectra at 358K) and start behaving as the isochronous methylene

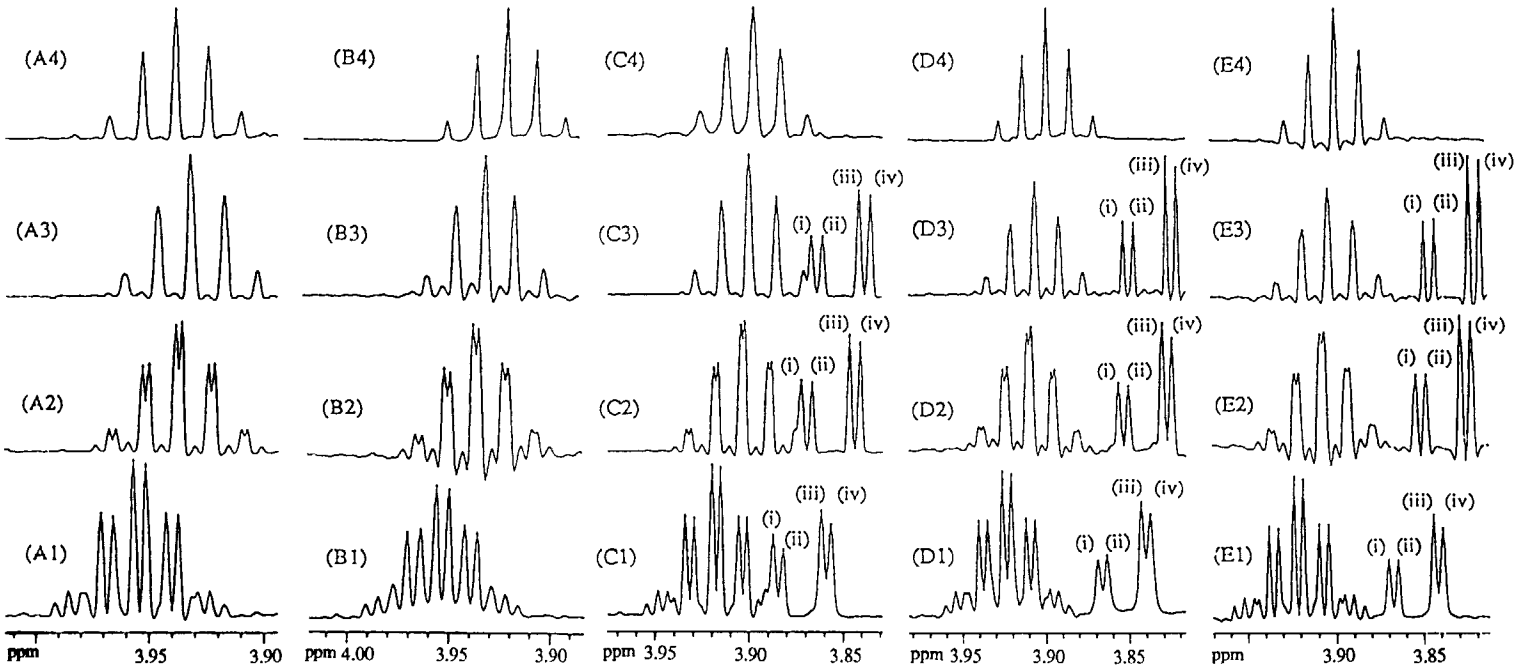

Figure 4. Expansions of 500 MHz ^{1}H-NMR spectra of methylene protons of 3'-ethylphosphate groups in ApEt (**21**) at 278 K [panel (A1)], at 318 K [panel (A2)] and at 358 K [panel (A3)] in comparison to dApEt (**16**) at 278 K [panel (A4)], in GpEt (**22**) at 278 K [panel (B1)], at 318 K [panel (B2)] and at 358 K [panel (B3)] compared to dGpEt (**17**) at 278 K [panel (B4)], in CpEt (**23**) at 278 K [panel (C1)], at 318 K [panel (C2)] and at 358 K [panel (C3)] compared to dCpEt (**18**) at 278 K [panel (C4)], in rTpEt (**24**) at 278 K [panel (D1)], at 318 K [panel (D2)] and at 358 K [panel (D3)] compared to TpEt (**19**) at 278 K [panel (D4)] and in UpEt (**25**) at 278 K [panel (E1)], at 318 K [panel (E2)] and at 358 K [panel (E3)] compared to dUpEt (**20**) at 278 K [panel (E4)]. In the case of CpEt (**23**) [panels (C1) - (C3)], rTpEt (**24**) [panel (D1) - (D3)] and UpEt (**25**) [panel (E1) - (E3)] signals of H5' [labeled (i) - (iv)] partly overlap with the multiplets of methylene protons.

protons (278 K - 358 K) of 2'-deoxynucleoside ethylphosphate counterparts[3d] (see panels A4, B4, C4, D4 & E4 of Fig. 4 for spectra at 278K), mimicking an unhindered motion of a rotor in the NMR time scale. *If the diminishing non-equivalence of the CH_2 protons at increasing temperature is caused by a shift of the conformational equilibria along ε, ζ or α torsion(s) then it should be attributed to the weakened interaction of the 2'-hydroxyl group with the vicinal heteroatom(s) as the temperature increases since we do not see any non-equivalence of CH_2 protons in 2'-deoxy-3'-ethylphosphate counterparts over the whole temperature range studied (278 - 358K).*[3d] Fourth, the intramolecular nature of 2'-OH interaction in **21** - **25** is also further evidenced by our observation of complete concentration-independent (from 50 mM to 1 mM range) chemical shifts ($\Delta\delta < 0.002$ ppm) and coupling constants ($\Delta J < 0.1$ Hz) at a particular temperature.

An alternative proposal of a direct H-bond between 2'-OH and one of the phosphate oxygen atoms in the (S,ε⁻) state of **21** - **25** was subsequently explored. We argued, if this cooperative conformational transitions of sugar repuckering and rotation of ε are also influencing other phosphate backbone torsions, such as α, ζ and β[14], to adopt certain preferred set of conformations. Such effect of cooperative sugar-ε motion in **21** - **25** is expected to be most felt on ζ (O3'-P) and α (P-O) torsions which are the closest to ε. There is however no J-coupling that would enable the conformational study of ζ and α torsions by NMR. We have therefore attempted to reorientate ζ and α torsions from trans to gauche⁻ or gauche⁺ region in a model building study (*vide infra*) and found that it is not possible to bring one of the 3'-phosphate oxygens to the vicinal 2'-OH any closer than 3.7 Å,[21d] which clearly showed that the rotation along ζ and α cannot give 2'-OH···phosphate-oxygen H-bond in (S,ε⁻) state.[21d] Furthermore, our molecular mechanics study[21d] on ApEt (**21**) has shown that (ζ⁻,α⁻) state in combination with (S,ε⁻) conformer is in fact the lowest in energy, but the distance between 2'-OH and one of the phosphate-oxygen atoms is 3.8 Å wheras the distance between 2'-OH and O3' is 2.1Å. Our model building studies with ApEt (**21**) furthermore suggests that 2'-OH can however form a H-bond with one of the phosphate-oxygens when C3'-O3' bond is rotated to ε^t state in S sugar conformation [d(2'-OH···O3')] = 2.4Å and [d(2'-OH···phosphate-oxygen)] = 1.9, 3.5 and 3.9Å]. In contrast, our experimental observation of the preferred ε⁻ state for C3'-O3' bond with S sugar conformation in ethylphosphates **21** - **25** suggests that the phosphate must be turned away from 2'-OH, thereby ruling out the possibility of any H-bonding between 2'-OH and one of the phosphate oxygen atoms.

Conclusion

(1) The 3'-phosphate group in ribonucleotides **11** - **15** drives N⇄S pseudorotational equilibria more to the S-type pseudorotamers than 3'-OH in ribonucleosides **1** - **5**, which is attributed to the fact that the gauche effect of O4'-C4'-C3'-3'-monophosphate fragment is stronger than that of O4'-C4'-C3'-3'OH. The increased drive towards S by the 3'-phosphate moiety is slightly dependent on the nature of the heterocyclic base and is larger in the case of pyrimidines ($\Delta\Delta H^\circ$ = -0.9 to -2.2 kJ mol^{-1}) than purines ($\Delta\Delta H^\circ$ = -0.3 and -1.3 kJ mol^{-1}). Note that the same trend was observed in 2'-deoxyribonucleoside 3'-monophosphates **6** - **10**.[3d] Our present thermodynamic data for N⇄S pseudorotational equilibria suggest that 3'-OPO_3Et^- group in **21** - **25** stabilizes the S-type pseudorotamers by -1.3 to -2.8 kJ mol^{-1} more compared to the corresponding 3'-phosphomonoesters **11** - **15**. The fact that as the population of ε^t rotamers in **21** - **25** increases, the population of S-type conformers decreases as the temperature is increased from 278 K to 358 K has led us to propose unique two-state (N,ε^t) ⇄ (S,ε⁻) conformational equilibrium. This means that the additional overall stabilization by 3'-OPO_3Et^- group in

21 - **25** compared to the corresponding 3'-phosphomonoesters **11** - **15** originates from the thermodynamic stabilization of the preferred ε orientation. The energetics for the drive of N⇄ S pseudorotational equilibrium (ΔH° and ΔS°) and $\varepsilon^t \rightleftarrows \varepsilon^-$ equilibrium ($\Delta H^\circ_\varepsilon$ and $\Delta S^\circ_\varepsilon$) in **21** - **25** are almost identical, which offers additional thermodynamic proof of the cooperativity in $(N,\varepsilon^t) \rightleftarrows (S,\varepsilon^-)$ conformational equilibria in these compounds.

(2) The unique interaction of 2'-OH with the vicinal heteroatom (*e.g.* O3') of the 3'-phosphate moiety acts as a molecular "On" switch between $(N,\varepsilon^t) \rightleftarrows (S,\varepsilon^-)$ conformational equilibria in **21** - **25**, whereas 2'-OH in a non-interacting state ("Off" switch) stabilizes the N and ε^t conformers in **21** - **25**. This 2'-OH interaction with the vicinal phosphate stabilizes the S and ε^- conformers in a cooperative manner over N and ε^t by $\Delta G^{298} \approx$ -2.8 kJ mol^{-1} for adenosine 3'-ethylphosphate (ApEt, **21**), -2.1 kJ mol^{-1} for guanosine 3'-ethylphosphate (GpEt, **22**), -0.9 kJ mol^{-1} for ribothymidine 3'-ethylphosphate (rTpEt, **14**) and -0.7 kJ mol^{-1} for uridine 3'-ethylphosphate (UpEt, **15**) (Table 2). The free-energy stabilization of S and ε^- conformers is relatively smaller (ΔG^{298} = 0.1 kJ mol^{-1}) for cytidine 3'-ethylphosphate (CpEt, **13**) because of the strongly opposing anomeric effect[3] [cytidine (5.2 kJ mol^{-1}) > uridine (4.5 kJ mol^{-1}) > ribothymidine (3.7 kJ mol^{-1}) > guanosine (3.1 kJ mol^{-1}) > adenosine (2.1 kJ mol^{-1})][3i], which stabilizes N-type sugar specially in the pyrimidine series.

(3) Since the in-line attack of 2'-OH to the vicinal phosphate in the RNA self-cleavage reaction[17] to give the 2',3'-cyclic phosphate through the transient trigonal bipyramidal phosphorane requires both S and ε^- conformers[16a-c], it means that the internucleotidyl phosphates of the pyrimidine nucleotide can relatively more easily take up that preferred S,ε^- conformation [energetic preference of the (S,ε^-) state over (N,ε^t) state for C **23** = 0.1 kJ mol^{-1}, for rT **24** = 0.9 kJ mol^{-1} and for U **25** = 0.7 kJ mol^{-1}] presumably because of much lower activation energy barrier for the two-state $(N,\varepsilon^t) \rightleftarrows (S,\varepsilon^-)$ conformational equilibria than those for the purine nucleotides [energetic preference of the (S,ε^-) state over (N,ε^t) state for A **21** = -2.8 kJ mol^{-1} and for G **22** = -2.1 kJ mol^{-1}]. In this regard, it is noteworthy that the catalytic RNA cleavage[17] in the hammerhead ribozyme is relatively more preferred (to give 2',3'-cyclic phosphate) when cytidine is at the self-cleavage site compared to any other nucleobase: C (100%), A (70%), U (5%) and G (<0.3%)[16d]. Furthermore, it should be noted that it is the uridine nucleotide in UA rich RNA sequence[15] that undergoes most frequent self-cleavage reaction.

(4) It may be noted that as a result of internucleotidyl stacking, the structural feature of double stranded RNA-RNA[1,18] and RNA-DNA[19] complex is dominated by the N-type sugar and ε^t-type orientation across C3'-O3' bond. On the other hand, when the internucleotidyl stacking is absent as in the central nucleotide residue of the single stranded hairpin loop[18], then the sugar is S-type, C4'-C5' rotamer is *gg* and ε is predominantly in ε^- state, which are all actually modelled[23] in our test systems **21** - **25**.

Experimentals

NMR Spectroscopy. ^{1}H- and ^{13}C-NMR one-dimensional spectra were recorded on Bruker AMX 500 spectrometer in D_2O between 278K and 358K in 10 K intervals at pH between 6.5 and 7.9. ^{1}H spectra have been recorded using 64K data points and 8 scans with ≈20 mM concentration for **1** - **5**, **11** - **15** and ≈50 mM for **21** - **25**. Almost negligible change in the chemical shift (< 0.1 ppm) of all protons over the whole temperature and concentration (1 mM - 50 mM) range suggests the absence of aggregation. ^{13}C-NMR spectra have been acquired for **21** - **25** using 128K data points resulting in the digital resolution of 0.17 Hz/point. The influence of the increase of digital resolution from the initial value of 0.17 Hz (obtained with SI = 128K) to 0.09 Hz upon increasing the value of SI to 256K did not result in any change of the magnitude of $^3J_{CP}$ over 278K - 358K. The measured $^3J_{CP}$ coupling constants for **21** - **25** extracted from the latter FT spectrum were identical to those reported in Table 1 (±0.3 Hz). This means that the experimentally observed change in the magnitude of $^3J_{CP}$ over 278K - 358K for **21** - **25** are not the result of the errors inherent in the measurement

procedure but correspond indeed to the actual change of the conformation along ε torsion. The proton chemical shifts and J_{HH} (error ± 0.08 Hz) were simulated and iterated by the DAISY program package (version 10.2c), which is a spin simulation and iteration program (upto seven spins) from Bruker. J_{HH} (±0.1 Hz) and J_{HP} (±0.1 Hz) were obtained after simulation of 1D ^{1}H-spectra. The precision of the J-values of CH_2 multiplet is slightly lower because these signals overlap with H5' for **23**. $^4J_{H2'P}$ of 0.5 Hz was estimated for **23** and **24** by the comparison of the linewidths of signals within the H2' multiplet in the experimental and simulated spectra.

Conformational analyses. The conformational analyses of $^3J_{HH}$ in **1** - **5**, **11** - **15** and **21** - **25** were performed by the PSEUROT (version 5.4) program[5b] which calculates best fit of experimental J-values to the five conformational parameters (P and Ψ_m for both N and S conformers and corresponding mole fractions). The following λ electronegativities were used for the substituents on H-C-C-H fragments in **1** - **5**, **11** - **15** and **21** - **25**: H 0.00, O4' and phosphate 1.27, OH 1.26, N of the bases 0.58, C1', C2', C3' and C4' 0.62 and C5' 0.68. The thermodynamics[3] of N ⇄ S equilibrium have been obtained from various van't Hoff plots based on the mole fractions of N and S conformers as obtained by several PSEUROT optimizations in which we have constrained the geometries of the minor pseudorotamer in such a way that a wide region of conformational hyperspace in terms of P (*i.e.* for N-type $0° < P_N < 36°$ and for S-type $144° < P_S < 190°$) and Ψ_m (30° - 46°) found in X-ray crystal structures of nucleos(t)ides is covered. The deviation between the experimental and back-calculated coupling constants, which are known function of the geometry of N and S as well as their respective population, is monitored in terms of r.m.s. error and maximum individual error of $^3J_{HH}$. Only the optimized geometries and populations with r.m.s. error below 0.3 Hz and maximum individual deviation between the experimental and back-calculated coupling constants below 0.6 Hz were accepted. The populations of N and S pseudorotamers at various temperatures from individual PSEUROT analyses are used to construct individual van't Hoff plots which give individual enthalpy and entropy value. Those are used to calculate average ΔH° and ΔS° and their respective standard deviations which are reported in Table 2.

$^3J_{C4'P}$, $^3J_{C2'P}$ and $^3J_{H3'P}$ of **21** - **25** measured at nine temperatures were interpreted with our computer program EPSILON in terms of the two-state $\varepsilon^t \rightleftarrows \varepsilon^-$ conformational equilibrium. The three-parameter Karplus equations[10,11] for $^3J_{CP} = 9.1\cos^2\Phi - 1.9\cos\Phi + 0.8$ and $^3J_{HP} = 15.3\cos^2\Phi - 6.2\cos\Phi + 1.5$ were used.

The program EPSILON finds the ε^t torsion, the ε^- torsion and the mole fraction of the ε^t rotamer (x_{ε^t}) which fit best with the given experimental $^3J_{C4'P}$, $^3J_{C2'P}$, and $^3J_{H3'P}$ coupling constants using a Metropolis algorithm[20] in conjunction with simulated annealing. In the Metropolis algorithm, a randomly proposed change of a variable is accepted with a probability (ρ) which is proportional to $\exp(-\Delta E/kT)$, where k is the Boltzmann constant, T is the temperature and E is the objective function which is beeing minimized. Changes where ΔE is negative are thus always accepted while changes to higher 'energy' levels of the objective function are accepted only with certain probability given by ρ. If the temperature T is lowered sufficiently slowly the system will reach its global minimum. In the program EPSILON, the objective function to be minimized is the r.m.s. error of the calculated *vs.* experimental coupling constants. The relationship between J_{calc} and the unknowns (ε^t, ε^-, x_{ε^t}) is:

$$J_{calc} = x_{\varepsilon^t} * (A * \cos^2(\varepsilon^t) + B * \cos(\varepsilon^t) + C) + (1 - x_{\varepsilon^t}) * (A * \cos^2(\varepsilon^-) + B * \cos(\varepsilon^-) + C).$$

The three sets of the Karplus parameters A, B, and C (one set for each of $^3J_{C4'P}$, $^3J_{C2'P}$ and $^3J_{H3'P}$) are entered by the user (the program also allows the Karplus parameters to be optimized, if so desired). For each compound, coupling constants for several temperatures can be entered and it is assumed that only the mole fraction is changing with temperature, not the values of ε^- and ε^t torsions. The torsions may of course differ between different compounds. Limits for maximum and minimum allowed values for the torsions can also be entered. The annealing scheme is also under user control, initial and final 'temperature' as well as the 'cooling' rate is entered by the user. The program is written in Fortran and tested on Silicon Graphics computers.

Acknowledgments. We thank Swedish Board for Technical Development (NUTEK), Swedish Natural Science Research Council (NFR) for generous financial supports and Uppsala University for funds for the purchase of a 500 MHz Bruker AMX NMR spectrometer.

References and Notes

1. Saenger, W. *Principles of Nucleic Acid Structure*, Springer Verlag, Berlin, **1988**.
2. Altona, C.; Sundaralingam, M. *J. Am. Chem. Soc.* **1972**, *94*, 8205; *ibid* **1973**, *95*, 2333.

3. (a) Plavec, J.; Tong, W.; Chattopadhyaya, J. *J. Am. Chem. Soc.* **1993**, *115*, 9734. (b) Plavec, J.; Garg, N.; Chattopadhyaya, J. *J. Chem.Soc., Chem. Commun.* **1993**, 1011. (c) Plavec, J.; Koole, L.H.; Chattopadhyaya, J. *J. Biochem. Biophys. Meth.* **1992**, *25*, 253. (d) Plavec, J.; Thibaudeau, C.; Viswanadham, G.; Sund, C.; Chattopadhyaya, J. *J. Chem. Soc., Chem. Comm.* **1994**, 781. (e) Thibaudeau, C.; Plavec, J.; Watanabe, K.A.; Chattopadhyaya, J. *J. Chem. Soc., Chem. Comm.* **1994**, 537. (f) Thibaudeau, C.; Plavec, J.; Garg, N.; Papchikhin, A.; Chattopadhyaya, J. *J. Am. Chem. Soc.* **1994**, *116*, 4038. (g) Plavec, J.; Thibaudeau, C.; Chattopadhyaya, J. *J. Am. Chem. Soc.* **1994**, *116*, 6558. (h) Thibaudeau, C.; Plavec, J.; Chattopadhyaya, J. *J. Am. Chem. Soc.* **1994**, *116*, 8033. (i) Plavec, J. Ph.D Thesis, Department of Bioorganic Chemistry, Uppsala University, Sweden, **1995**.
4. (a) Olsthoorn, C.S.M.; Doornbos, J.; de Leeuw, H.P.M.; Altona, C. *Eur. J. Biochem.* **1982**, *125*, 367. (b) Birnbaum, G.I.; Giziewicz, J.; Huber, C.P.; Shugar, D. *J. Am. Chem. Soc.* **1976**, *98*, 4640. (c) Izatt, R.M.; Hansen, L.D.; Rytting, J.H.; Christensen, J.J. *J. Am. Chem. Soc.* **1965**, *87*, 2760. (d) Bolton, P.H.; Kearns, D.R. *Biochim. Biophys. Acta* **1978**, *517*, 329. (e) Bolton, P.H.; Kearns, D.R. *J. Am. Chem. Soc.* **1979**, *101*, 479.
5. (a) Altona, C.; Ippel, J.H.; Hoekzema, A.J.A.W.; Erkelens, C.; Groesbeek, G.; Donders, L.A. *Magn. Reson. Chem.* **1989**, *27*, 564. (b) de Leeuw, F.A.A.M. and Altona, C. *J. Comp Chem.* **1983**, *4*, 428. (c) van Wijk, J.; Huckriede, B.D.; Ippel, J.H.; Altona, C. *Methods Enzymol.* **1992**, *211*, 286.
6. Three endocyclic coupling constants ($^3J_{H1'-H2'}$, $^3J_{H2'-H3'}$ and $^3J_{H3'-H4'}$) in **1 - 5**, **11 - 15** and **21 - 25** measured in the temperature range 278 K - 358 K at 10 K intervals were analysed by the PSEUROT[5b] program which calculates their best fit to the five conformational parameters (P and Ψ_m for both N and S conformers and corresponding mole fractions). As three observables can not define five unknowns the geometries of minor N conformers had to be kept fixed in the range $-36° < P_N < +36°$ in 18° steps and alternatively, when there is no high preference for S-type pseudorotamers Ψ_m of both N and S type pseudorotamers were fixed in the range $30° < \Psi_m < 40°$ in 1° steps. Several PSEUROT optimizations of $^3J_{HH}$ in **1 - 5**, **11 - 15** and **21 - 25** gave low r.m.s. error (< 0.2 Hz) and small individual deviations between experimental and calculated $^3J_{HH}$ (< 0.4 Hz). The resulting populations from individual PSEUROT analyses were used to make van't Hoff plots[3] (Fig. 1) in order to calculate $\Delta H°$ and $\Delta S°$ which were used to calculate the average $\Delta H°$ and $\Delta S°$ (for their signs see footnote 'a' of Table 2) of N $\rightleftarrows$ S equilibria in **1 - 5**, **11 - 15** and **21 - 25** and their associated standard deviations presented in Table 2.
7. (a) Lankhorst, P.P.; Haasnoot, C.A.G.; Erkelens, C.; Altona, C. *J. Biomol. Struct. Dyn.* **1984**, *1*, 1387. (b) Blonski, W.J.P.; Hruska, F.E.; Sadana, K.L.; Loewen, P.C. *Biopolymers* **1983**, *22*, 605. (c) Alderfer, J.L.; Ts'o, P.O.P. *Biochemistry* **1977**, *16*, 2410. (d) Davies, D.B.; Sadikot, H. *Biopolymers* **1983**, *22*, 1843.
8. Blommers, M.J.J.; Nanz, D.; Zerbe, O. *J. Biomol. NMR* **1994**, *4*, 595.
9. The values of $^4J_{H2'P}$ can be used to qualitatively assess[8] the population of ε^- rotamers: 65% at 278 K, 61% at 318 K and 43% at 358 K for **21**, 52% at 278 K, 48% at 318 K and 48% at 358 K for **22** and 30% at 278 K, 30% at 318 K and 22% at 358 K for **25**. In **23** and **24** $^4J_{H2'P}$ was not resolved (see footnote in Table 1) and the estimated value of 0.5 Hz corresponds to 22% of ε^- rotamers.
10. Plavec, J. and Chattopadhyaya, J. *Tetrahedron Lett.* **1995**, *36*, 1949.
11. Mooren, M.M.W.; Wijmenga, S.S.; van der Marel, G.A.; van Boom, J.H.; Hilbers, C.W. *Nucl. Acids Res.* **1994**, *22*, 2658.
12. Dhingra, M.M.; Saran, A. *Biopolymers* **1982**, *21*, 859.
13. The 15 independent calculations with program EPSILON in which ε^t and ε^- torsion angles and their respective populations were varied to obtain the best fits between 27 experimental $^3J_{C4'P}$, $^3J_{C2'P}$ and $^3J_{H3'P}$ coupling constants in 278 - 358 K temperature range in each of **21 - 25** and calculated J values (maximum $\Delta J < 1.1$ Hz with the r.m.s. = 0.5 Hz) resulted in the following conformational equilibria: $[193° \le \varepsilon^t \le 221°$, 23% ($\sigma$ = 5%) at 278K, 38% (σ = 5%) at 358K$] \rightleftarrows [258° \le \varepsilon^- \le 270°]$ for **21**, $[193° \le \varepsilon^t \le 215°$, 25% ($\sigma$ = 5%) at 278K, 38% (σ = 6%) at 358K$] \rightleftarrows [257° \le \varepsilon^- \le 268°]$ for **22**, $[195° \le \varepsilon^t \le 223°$, 45% ($\sigma$ = 13%) at 278K, 52% (σ = 12%) at 358K$] \rightleftarrows [252° \le \varepsilon^- \le 282°]$ for **23**, $[188° \le \varepsilon^t \le 215°$, 36% ($\sigma$ = 6%) at 278K, 42% (σ = 6%) at 358K$] \rightleftarrows [252° \le \varepsilon^- \le 267°]$ for **24** and $[199° \le \varepsilon^t \le 214°$, 36% ($\sigma$ = 4%) at 278K, 44% (σ = 6%) at 358K$] \rightleftarrows [257° \le \varepsilon^- \le 267°]$ for **25**. The changes in the population of ε^t rotamers in **21 - 25** at other temperatures are plotted Fig. 2.

14. The decrease of β^t population is evident from the decrease in $^3J_{\underline{C}H_3P}$ by 0.4 - 0.5 Hz in 11 - 15 with the increase of temperature from 278 to 358 K (Table 1). The populations of β^t rotamers at three different temperatures calculated by relation[7a] $\%\beta^t = [25.5 - \Sigma(^3J_{CH_2P})]*100/20.5$ are: 55% at 278 K, 53% at 318 K and 52% at 358 K for **21**, 56% at 278 K, 53% at 318 K and 50% at 358 K for **22**, 56% at 278 K, 52% at 318 K and 52% at 358 K for **23**, 55% at 278 K, 53% at 318 K and 50% at 358 K for **24** and 55% at 278 K, 53% at 318 K and 50% at 358 K for **25**.
15. (a) Kierzek, R. *Nucl. Acids Res.* **1992**, *20*, 5073. (b) *ibid* **1992**, *20*, 5079. (c) Capaldi, D.C.; Reese, C.B. *Nucl. Acids Res.* **1994**, *22*, 2209.
16. (a) Agback, P.; Glemarec, C.; Yin, L.; Sandström, A.; Plavec, J.; Sund, C.; Yamakagem S-I.; Viswanadham, G.; Rousse, B.; Puri, N.; Chattopadhyaya, J. *Tetrahedron Letts.* **1993**, *34*, 3929. (b) Rousse, B.; Puri, N.; Viswanadham, G.; Agback, P.; Glemarec, C.; Sandström, A.; Sund, C.; Chattopadhyaya, J. *Tetrahedron* **1994**, *50*, 1777. (c) Rousse, B.; Sund, C.; Glemarec, C.; Sandström, A.; Agback, P.; Chattopadhyaya, J. *Tetrahedron* **1994**, *50*, 8711. (d) Ruffner, D.E., Stormo, G.D., Uhlenbeck, O.C. *Biochemistry* **1990**, *529*, 10695.
17. (a) Uhlenbeck, O.C. *Nature* **1987**, *328*, 596. (b) Ruffner, D.E.; Stormo, G.D.; Uhlenbeck, O.C. *Biochemistry* **1990**, *29*, 10695. (c) Pieken, W.A.; Olsen, D.B.; Benseler, F.; Aurup, H.; Eckstein, F. *Science* **1991**, *253*, 314. (d) Williams, D.M.; Pieken, W.A.; Eckstein, F. *Proc. Natl. Acad. Sci. USA* **1992**, *89*, 918. (e) Haseloff, J.; Gerlach, W.L. *Nature* **1988**, *334*, 585. (f) Jeffries, A.C.; Symons, R.H. *Nucl. Acids Res.* **1989**, *17*, 1371.
18. Varani, G.; Cheong, C.; Tinoco, I. *Biochemistry* **1991**, *30*, 3280.
19. Maltseva, T.V.; Agback, P.; Repkova, M.N.; Venyaminova, A.G.; Ivanova, E.M.; Sandström, A.; Zarytova, V.F.; Chattopadhyaya, J. *Nucl. Acids Res.* **1994**, *22*, 5590.
20. Press, W.H.; Flannery, B.P.; Tenkolsky, S.A.; Vetterling, W.T. *Numerical Recipes (Fortran version)*, Cambridge University Press, New York, **1990**.
21. (a) Still, W.C. *et al.*, MacroModel V3.5a, **1992**, Columbia University, New York. (b) Mohamadi, F.; Richards, N.G.J.; Guida, W.C.; Liskamp, R.; Lipton, M.; Caufield, C.; Chang, G.; Hendrickson, T.; Still, W.C. *J. Comp. Chem.* **1990**, *11*, 440. (c) Weiner, S.J.; Kollman, P.A.; Nguyen, D.T.; Case, D.A. *J. Comp. Chem.* **1986**, *7*, 230. (d) An all atom AMBER force field[21c] as implemented in MacroModel program[21a,b] has been used to understand the implication of different preferred rotamer of α and ζ in (S,ε⁻) state on the possibility of a potential H-bond between 2'-OH and one of the phosphate oxygens. The Coulombic electrostatic and van der Waals nonbonding cutoffs were both set to 25Å, which exceeds the size of ApEt (**21**). Dielectric constant in the distance-dependent electrostatics treatment was set to 4r. Charges on the individual atoms were assigned by the MacroModel program.[21a-c] Nine starting conformers of ApEt (**21**) in the (S,ε⁻) state with ζ and α independently placed at 60°, 180° and 300° were freely energy minimized to derivative convergence of 0.004 kJ mol^{-1} $Å^{-1}$. All the energy minimized structures showed the following structural characteristics (with a constant distance between 2'-O<u>H</u> and O3' of 2.1Å): (1) S (P = 139° , Ψ_m = 43°), γ = 58°, ε = 276°, ζ = 288°, α = 293° , β = 179° and d(2'-O<u>H</u>···phosphate-oxygens) = 3.8, 4.0 & 4.8Å); E_{tot} = 10.8 kJ mol^{-1}; (2) S (P = 142° , Ψ_m = 43°), γ = 58°, ε = 286°, ζ = 89°, α = 66° , β = 182° and d(2'-O<u>H</u>···phosphate-oxygens) = 3.8, 4.4 & 4.5Å); E_{tot} = 13.3 kJ mol^{-1}; (3) S (P = 143° , Ψ_m = 42°), γ = 58°, ε = 279° , ζ = 264°, α = 66°, β = 176° and d(2'-O<u>H</u>···phosphate-oxygens) = 3.7, 4.2 & 4.6Å); E_{tot} = 14.0 kJ mol^{-1}; (4) S (P = 138° , Ψ_m = 43°), γ = 58°, ε = 277° , ζ = 287°, α = 180°, β = 180° and d(2'-O<u>H</u>···phosphate-oxygens) = 3.8, 4.0 & 4.7Å); E_{tot} = 16.6 kJmol^{-1}; (5) S (P = 135° , Ψ_m = 43°), γ = 59°, ε = 277° , ζ = 172° and α = 292° , β = 179° and d(2'-O<u>H</u>···phosphate-oxygens) = 3.9, 3.9 & 4.7Å); E_{tot} = 16.9 kJ mol^{-1}; (6) S (P = 134° , Ψ_m = 43°), γ = 59°, ε = 277°, ζ = 178°, α = 68°, β = 181° and d(2'-O<u>H</u>···phosphate-oxygens) = 3.8, 4.0 & 4.6Å); E_{tot} = 17.0 kJ mol^{-1}; (7) S (P = 126°, Ψ_m = 44°), γ = 60°, ε = 278°, ζ = 69°, α = 182°, β = 180° and d(2'-O<u>H</u>···phosphate-oxygens) = 3.9, 4.2 & 4.6Å); E_{tot} = 18.7 kJ mol^{-1}; (8) S (P = 153° , Ψ_m = 41°), γ = 59°, ε = 267° , ζ = 63°, α = 253°, β = 174° and d(2'-O<u>H</u>···phosphate-oxygens) = 3.8, 3.9 & 4.6Å); E_{tot} = 20.4 kJ mol^{-1}; (9) S (P = 134° , Ψ_m = 43°), γ = 59°, ε = 277° , ζ = 177°, α = 180° , β = 180° and d(2'-O<u>H</u>···phosphate-oxygens) = 3.8, 4.0 & 4.6Å); E_{tot} = 22.4 kJ mol^{-1}.
22. (a) Birnbaum, G.I.; Giziewicz, J.; Huber, C.P.; Shugar, D. *J. Am. Chem. Soc.* **1976**, *98*, 4640. (b) Munns, A.R.I.; Tollin, P. *Acta Cryst.* **1970**, *B26*, 1101. (c) Cucruix, A.; Riche, C.; Pascard, C. *Acta Cryst.* **1976**, *B32*, 2467. (d) Narayanan, P.; Berman, H.M. *Carbohydrate Res.* **1975**, *44*, 169. (e) Izatt, R.M.; Hansen,

L.D.; Rytting, J.H.; Christensen, J.J. *J. Am. Chem. Soc.* **1965**, *87*, 2760. (f) Jeffrey, G.A.; Takagi, S. *Acc. Chem. Res.* **1978**, *11*, 264.

23. (a) In **21** - **25**, γ torsions were found to be in equilibrium amongst three staggered conformers (γ^+) ⇄ (γ^-) ⇄ (γ^t), but the γ^+ is overwhelmingly preferred[23b] at all temperatures used for monitoring $^3J_{H4'/H5'}$ and $^3J_{H4'/H5''}$ [2.4, 3.1 Hz at 278K (81% γ^+) and 3.0, 4.0 Hz at 358K (66% γ^+) for ApEt **21**; 2.7, 3.7 Hz at 278K (72% γ^+) and 3.2, 4.5 Hz at 358K (59% γ^+) for GpEt **22**; 2.6, 4.1 Hz at 278K (68% γ^+) and 3.0, 4.6 Hz at 358K (59% γ^+) for CpEt **23** ; 2.8, 4.0 Hz at 278K (68% γ^+) and 3.1, 4.5 Hz at 358K (60% γ^+) for rTpEt **24** and 2.7, 4.1 Hz at 278K (67% γ^+) and 3.1, 4.6 Hz at 358K (59% γ^+) for UpEt **25**)]. Also a simple comparison of $^3J_{H4'/H5'}$ and $^3J_{H4'/H5''}$ at 25°C for our model compunds **21**- **25** (2.6 & 3.3 Hz for ApEt **21**, 2.9 & 3.9 Hz for GpEt **22**, 2.8 & 4.3 Hz for CpEt **23** and 2.8 & 4.3 Hz for UpEt **25**) with those of the nucleotides in the single-stranded RNA hairpin loop region at 25°C [≈4 & ≈3 Hz for U_4, <3 & <3 Hz for U_5 and ≈5 & ≈3 Hz for U_6 reported by Tinocco et al in *Nucleic Acid Res*, **21**, 537-545 (1993), and <3 & <3 Hz for U_5, 3.5 & 3 Hz for U_6 and <3 & 3 Hz for C_7 reported by Tinocco et al in *Biochemistry*, **30**, 3280-3289 (1991)] shows that the conformation of the preferred *gg* rotamer in our model compounds is closely similar to what is found for the nucleotides in the single-stranded hairpin of RNA. This means that the total stabilization of the S conformer by 2.5-3.8 kJ mol^{-1} in our model compounds, compared to the corresponding 3'-OH counterparts **1**- **5** , is the result of both the preferred *gg* orientation of O5' as well as the gauche effect of the 3'-ethylphosphate, which are the conformational features also found in the single stranded hairpin region of RNA. This leads us to conclude that the conformational behaviour of compounds **21** - **25** are adequate models for the nucleotides in the single-stranded hairpin of RNA. It should be also however noted that whether C5' has a hydroxyl or a phosphate group has no influence on the N ⇄ S pseudorotational equilibrium (ref. 4a). Hence, the modelling of the sugar and the 3'-phosphodiester conformational equilibria as exist in the single-stranded RNA region remain to be valid. (b) Haasnoot, C.A.G.; de Leeuw, F.A.A.M.; de Leeuw, H.P.M.; Altona, C. *Recl. Trav. Chim. Pays-Bas* **1979**, *98*, 576.

24. The observed energetics of interaction of 2'-OH group with the vicinal 3'-ethylphosphate moiety based on the subtraction of energetics of ribonucleoside 3'-monophosphates from the corresponding 3'-ethylphosphates has been also found to be quite *consistent* with independent dissection of the energetics of interaction of 2'-OH group with the vicinal 3'-ethylphosphate moiety from the other 2'-OH promoted gauche effects (ref. 3a) basing on the following two sets of comparisons: (i) the pairwise comparison between the pairs of ribonucleoside-3'-ethylphosphates **21** - **25** and their 2'-deoxy counterparts **16** - **20** gave $\Delta\Delta H^\circ_1$ = -1.4 kJ mol^{-1} and $\Delta\Delta G^\circ_1$ = +0.3 kJ mol^{-1} for the pair dApEt (**16**) / ApEt (**21**); $\Delta\Delta H^\circ_1$ = -1.0 kJ mol^{-1} and $\Delta\Delta G^\circ_1$ = -1.0 kJ mol^{-1} for the pair dGpEt (**17**) / GpEt (**22**); $\Delta\Delta H^\circ_1$ = +2.1 kJ mol^{-1} and $\Delta\Delta G^\circ_1$ = +2.1 kJ mol^{-1} for the pair dCpEt (**18**) / CpEt (**23**); $\Delta\Delta H^\circ_1$ = +0.5 kJ mol^{-1} and $\Delta\Delta G^\circ_1$ = +1.1 kJ mol^{-1} for the pair TpEt (**19**) / rTpEt (**24**) and $\Delta\Delta H^\circ_1$ = +1.1 kJ mol^{-1} and $\Delta\Delta G^\circ_1$ = +1.3 kJ mol^{-1} for the pair dUpEt (**20**) / CpEt (**25**). (ii) The pairwise comparison between the pairs of ribonucleoside-3'-monophosphates **11** - **15** and their 2'-deoxy counterparts **6** - **10** gave $\Delta\Delta H^\circ_2$ = +0.5 kJ mol^{-1} and $\Delta\Delta G^\circ_2$ = +0.2 kJ mol^{-1} for the pair dAMP (**6**) / AMP (**11**); $\Delta\Delta H^\circ_2$ = -0.4 kJ mol^{-1} and $\Delta\Delta G^\circ_2$ = +0.9 kJ mol^{-1} for the pair dGMP (**7**) / GMP (**12**); $\Delta\Delta H^\circ_2$ = +4.0 kJ mol^{-1} and $\Delta\Delta G^\circ_2$ = +2.2 kJ mol^{-1} for the pair dCMP (**8**) / CMP (**13**); $\Delta\Delta H^\circ_2$ = +1.7 kJ mol^{-1} and $\Delta\Delta G^\circ_2$ = +1.7 kJ mol^{-1} for the pair TMP (**9**) / rTMP (**14**) and $\Delta\Delta H^\circ_2$ = +3.9 kJ mol^{-1} and $\Delta\Delta G^\circ_2$ = +2.2 kJ mol^{-1} for the pair dUMP (**10**) / UMP (**15**). The pairwise subtraction of the respective $\Delta\Delta H^\circ_2$ from $\Delta\Delta H^\circ_1$ values ($\Delta\Delta H^\circ_3 = \Delta\Delta H^\circ_1 - \Delta\Delta H^\circ_2$) and $\Delta\Delta G^\circ_2$ from $\Delta\Delta G^\circ_1$ values ($\Delta\Delta G^\circ_3 = \Delta\Delta G^\circ_1 - \Delta\Delta G^\circ_2$) for each nucleobase gives an independent assessment of strength of the interaction of 2'-OH with the 3'-ethylphosphate in **21** - **25**: $\Delta\Delta H^\circ_3$ = -1.9 kJ mol^{-1} and $\Delta\Delta G^\circ_3$ = +0.1 kJ mol^{-1} for adenine, $\Delta\Delta H^\circ_3$ = -0.6 kJ mol^{-1} and $\Delta\Delta G^\circ_3$ = -0.3 kJ mol^{-1} for guanine, $\Delta\Delta H^\circ_3$ = -1.9 kJ mol^{-1} and $\Delta\Delta G^\circ_3$ = -0.1 kJ mol^{-1} for cytosine, $\Delta\Delta H^\circ_3$ = -1.2 kJ mol^{-1} and $\Delta\Delta G^\circ_3$ = -0.6 kJ mol^{-1} for thymine and $\Delta\Delta H^\circ_3$ = -2.8 kJ mol^{-1} and $\Delta\Delta G^\circ_3$ = -0.9 kJ mol^{-1} for uracil.

(*Received in UK* 24 *July* 1995; *accepted* 1 *September* 1995)